Environ Geochem Health
https://doi.org/10.1007/s10653-021-01067-x

ORIGINAL PAPER

Epithelial morphometric alterations and mucosecretory responses in the nasal cavity of mice chronically exposed to hydrothermal emissions

R. Camarinho · A. Madrero Pardo · P. V. Garcia · A. S. Rodrigues

Received: 4 November 2020 / Accepted: 5 August 2021

Abstract Air pollutants (either of natural or anthropogenic origin) represent a considerable environmental risk to human health by affecting the respiratory system and causing respiratory disorders. In this study, we investigate the effects of chronic exposure to hydrothermal emissions on the nasal cavity of mice since it is the first and the most exposed region of the respiratory system. This study, carried in S. Miguel Island, Azores—Portugal, used *Mus musculus* as a bioindicator species. Mice were captured in an area with non-eruptive active volcanism (Furnas Village) and another area without volcanism (Rabo de Peixe, reference site). The hydrothermal emissions present at Furnas Village are characterized by the continuous release of several gases (CO_2, H_2S, ^{222}Rn) along with metals (e.g. Hg, Cd, Zn, Al) and particulate matter into the environment. We test the hypothesis whether chronic exposure to this specific type of pollution causes epithelial morphometric, mucosecretory and neuronal alterations on the nasal cavity. Thickness measurements were taken in the squamous, respiratory and olfactory epithelia. The relative density of cell types (basal, support and neurons) was also assessed in the olfactory epithelium and the mucosecretory activity was determined in the lateral nasal glands, Bowman's gland and goblet cells. Mice chronically

Capsule Chronic exposure to hydrothermal emissions causes epithelial and mucosecretory alterations in the nasal cavity.

Supplementary Information The online version contains supplementary material available at https://doi.org/10.1007/s10653-021-01067-x.

R. Camarinho · P. V. Garcia · A. S. Rodrigues (✉)
Faculty of Sciences and Technology, University of the Azores, 9501-801 Ponta Delgada, Portugal
e-mail: armindo.s.rodrigues@uac.pt

R. Camarinho
e-mail: Ricardo.AD.Camarinho@uac.pt

P. V. Garcia
e-mail: Patricia.V.Garcia@uac.pt

R. Camarinho · A. S. Rodrigues
IVAR Instituto de Vulcanologia e Avaliação de Riscos, University of the Azores, 9501-801 Ponta Delgada, Portugal

A. M. Pardo
Faculty of Biology, University of Barcelona, 08028 Barcelona, Spain
e-mail: amadrepa23@alumnes.ub.edu

P. V. Garcia
cE3c, Centre for ecology, Evolution and Environmental Changes/Azorean Biodiversity Group, University of the Azores, 9501-801 Ponta Delgada, Azores, Portugal

Published online: 26 August 2021

exposed to hydrothermal emissions presented thinner olfactory epithelia and lesser mucous production, which could result in loss of olfactory capabilities as well as a decrease in the protective function provided by the mucous to the lower respiratory tract. For the first time, it is demonstrated that, in mice, this specific type of non-eruptive active volcanism causes epithelial and mucosecretory alterations, leading to the loss of olfactory capabilities.

Keywords Air pollution · *Mus musculus* · Non-eruptive volcanism · Hydrothermal emissions · Nasal cavity · Histomorphometry

Abbreviations

AB/PAS	Alcian Blue (2.5 pH)/ Periodic Acid Schiff
GEM	Gaseous Elemental Mercury
BowGl	Bowman's Gland
GobCell	Goblet Cell
H&E	Haematoxylin and Eosin
LaNaGl	Lateral Nasal Gland
OlfEpi	Olfactory Epithelium
ResEpi	Respiratory Epithelium
SquEpi	Squamous Epithelium
VomOrg	Vomeronasal Organ
FOI	Functional Olfactory Index
FR	Furnas (Figures only)
RP	Rabo de Peixe (Figures only)

Introduction

Air pollution is a worldwide phenomenon recognized by the governmental authorities as a major public problem and a growing environmental concern to human health (Maynard et al., 2017). This growing concern includes air pollutants of anthropogenic and natural origin. Among the later, worldwide volcanoes, by yearly emitting around 150 million tons of carbon dioxide (CO_2) and other air contaminants (Amaral & Rodrigues, 2011), represent an important environmental risk with an unknown health impact to the 10% of the human population that inhabit areas with active volcanism (Hansel and Oppenheimer, 2004).

The Azorean archipelago (Portugal) is located in the North Atlantic Ocean, where the Eurasian, African and American lithospheric plates meet (Fig. 1a) (Searle, 1980). Because of this tectonic scenario (Fig. 1b), the island of S. Miguel is volcanically active and has three major active central volcanoes (Sete Cidades, Fogo and Furnas) (Guest et al., 1999). The volcanic complex of Furnas (Fig. 1c, d) is in the eastern part of the island. In this volcanic complex, volcanic activity is characterized by the occurrence of several hydrothermal emissions (non-eruptive volcanic manifestations). The hydrothermal emissions include phenomena like soil diffuse degassing, hot and cold CO_2-rich water springs and active fumarolic fields (Viveiros et al., 2010). Among the gaseous emission, it is possible to find large amounts of CO_2 [around 1000 tons per day (Viveiros et al., 2010)], hydrogen sulphide (H_2S), hydrogen fluoride (HF), the radioactive gas radon (^{222}Rn) (Silva et al., 2015) and GEM (Gaseous Elemental Mercury) (Bagnato et al., 2018). Exposure to the asphyxiant gas CO_2 has been proven to be related to increased inflammatory processes (Coakley et al., 2002). Radon is considered the main source of human exposure to any type of radioactivity (Hendry et al., 2009), and although considered to be the second leading cause of lung cancer by IARC (IARC, 1988), only recently a few studies have focused on ^{222}Rn exposure and its associated health risks in hydrothermal regions (Kristbjornsdottir & Rafnsson, 2013; Linhares et al., 2015, 2017). Exposure to GEM has been previously linked to neuropathologies (Navarro-Sempere et al., 2020). Most of these studies have been performed either in human populations or mice from Furnas volcanic complex. Inhabiting this volcanically active environment has proven to cause: in humans, DNA damage (Linhares et al., 2018; Rodrigues et al., 2012), respiratory dysfunctions (Linhares et al., 2015), higher risk of several types of cancer (Amaral et al., 2006) and chronic bronchitis (Amaral et al., 2007a); and in

Fig. 1 Map of the Azores Archipelago. **a** Location of the Azores archipelago in the Atlantic Ocean; **b** morphotectonic features and geographical groups of the Azores archipelago—red line defines approximately the separation of each plate based on the morphological expression of each structure; **c** map of S. Miguel Island and study area; **d** map of the volcanic complex of Furnas. Basemap aerial view backgrounds by ESRI ArcGIS online. "World Imagery" [basemap]. "World Imagery Map". Last updated 11/06/2020. https://www.arcgis.com/home/item.html?id=10df2279f9684e4a9f6a7f08febac2a9. Attribution information to both ESRI and other data providers shown in the figure

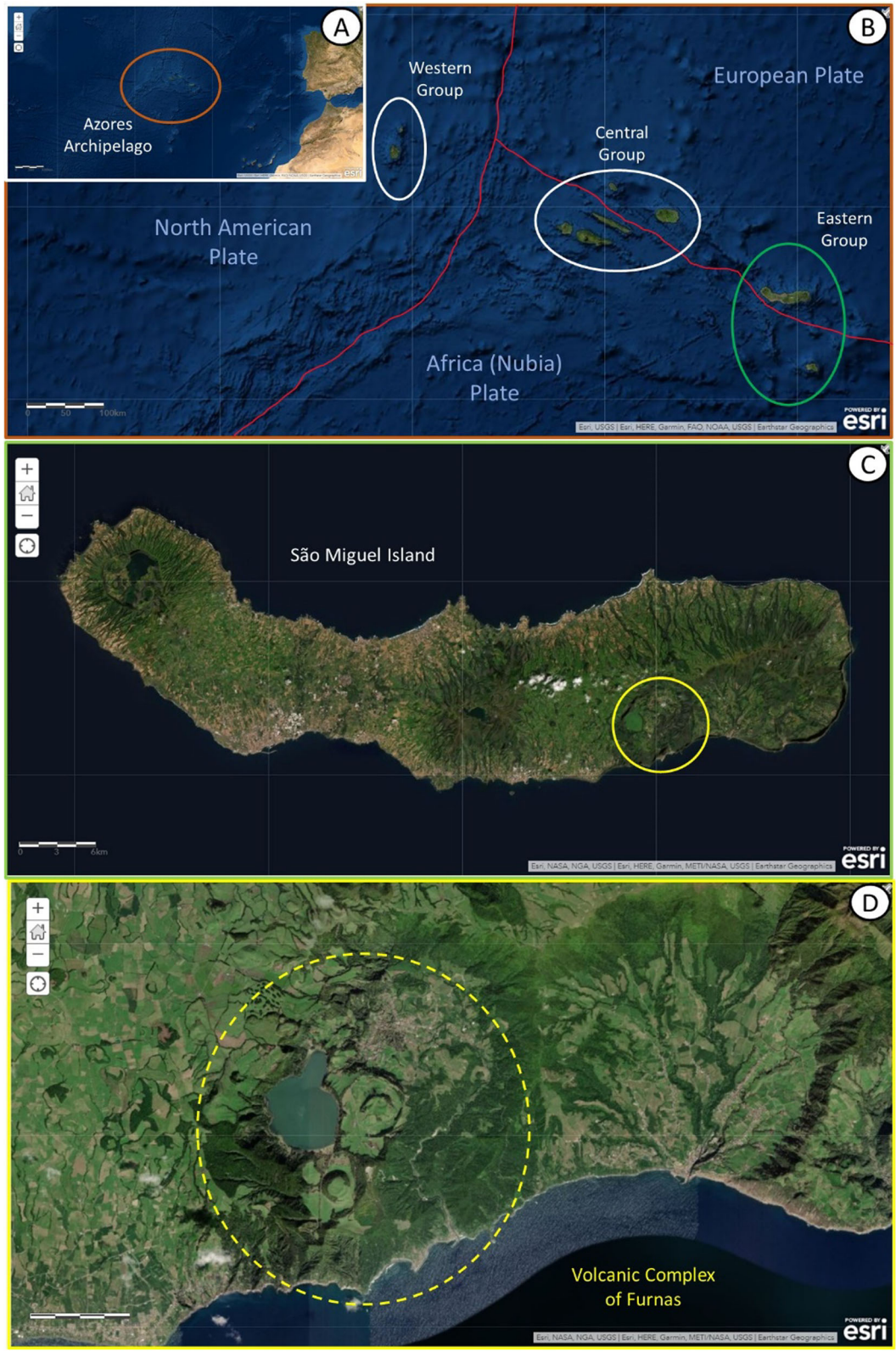
A
Azores
Archipelago
B
Western
Group
European Plate
Central
Group
Eastern
Group
North American
Plate
Africa (Nubia)
Plate
C
São Miguel Island
D
Volcanic Complex
of Furnas

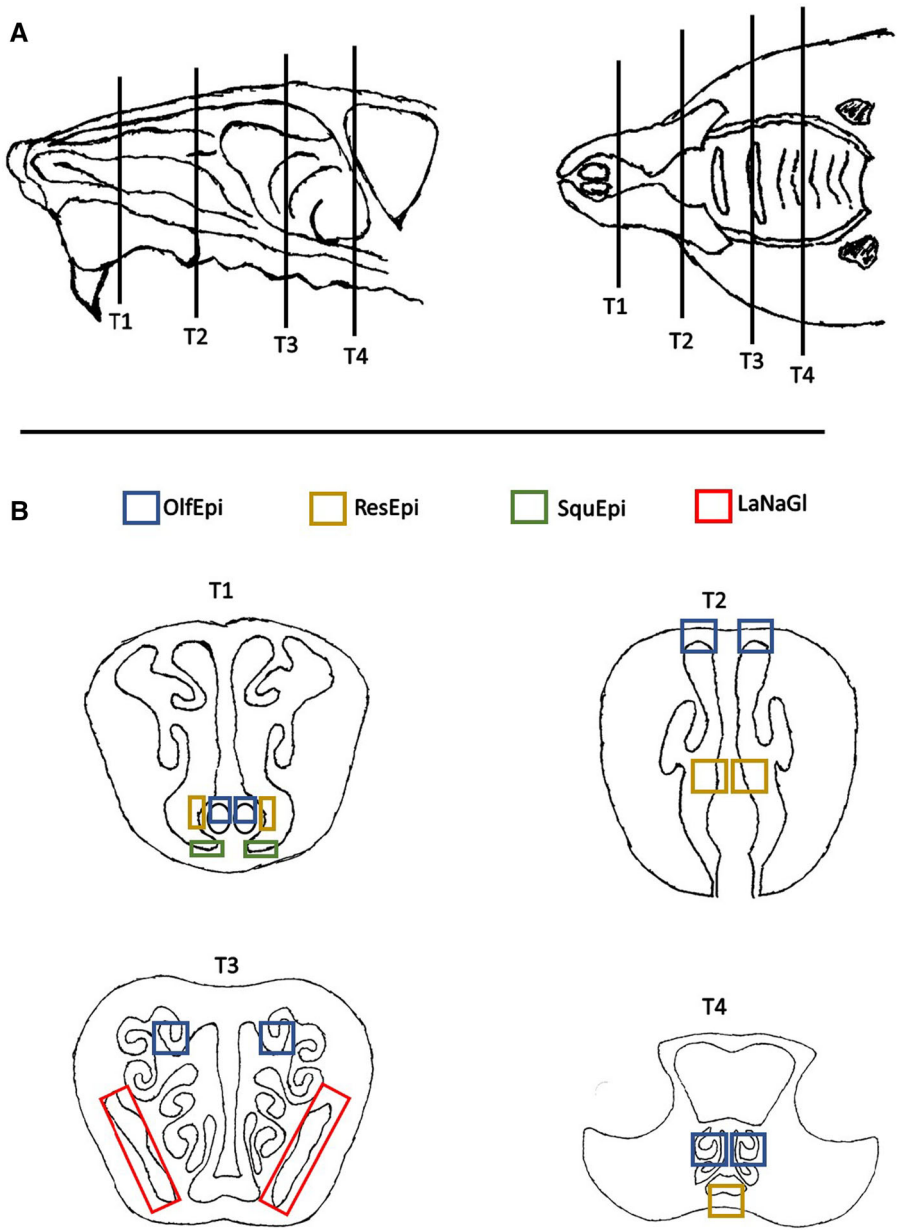

Fig. 2 Schematic representation mice nasal cavity and of the studied sections (T1–4): **a** right nasal passage of the mice nose with septum removed; **b** ventral view of the mice hard palate region, with the lower jaw removed; lines represent indicate surfaces of transverse tissue blocks (T1–4) that were selected for microscopy examination; **c** cross-sectional representation of T1–4; OlfEpi—olfactory epithelium, ResEpi—respiratory epithelium, SquEpi—squamous epithelium, LaNaGl—lateral nasal glands. Drawings and schematics based on the works of Corps et al., 2010 and Young et al., 1981)

mice, increased levels of heavy metals in the lungs, kidneys and liver (Amaral et al., 2007b), lung injury and lung structural remodelling (Camarinho et al., 2013, 2019a) and, pulmonary lesions consistent with asthma and chronic bronchitis (Camarinho et al., 2019b). These studies evidence the necessity to further explore the hazardous effects of chronic exposure to hydrothermal emissions, its pollutants and their ability to act synergistically. The above-mentioned studies in mice were mainly focused on the hazardous effects on the lower respiratory tract; hence, it is imperative to study the upper respiratory tract to fully understand

how this specific type of air pollution affects the whole respiratory system.

The hazardous effects of chronic exposure to hydrothermal emissions on the nasal cavity have never been reported. Therefore, the purpose of this study is to characterize the histological effects on the nasal epithelium and glands of *Mus musculus* (the chosen bioindicator species) chronically exposed to the hydrothermal emissions in the volcanically active location of Furnas (Azores—Portugal).

Materials and methods

Study design and mice populations

Two sets of *M. musculus* were live-captured (using live-catch mousetraps) at two different locations: one village with hydrothermal emissions (Furnas Village, $n = 10$) and another village without any type of volcanic activity (Rabo de Peixe Village, $n = 20$). The study location, volcanic characteristics, main hydrothermal emissions and the reason of choice to use *Mus musculus* as a bioindicator species have been previously described in detail by Camarinho et al. (2019a, b).

Animal necropsies and tissue processing

The live caught mice were weighted, gender identified and then euthanized. Mice age was calculated following the methodology of Quéré and Vincent (1989). Mice euthanization was performed ensuring a painless death with the use of isoflurane. Right after the euthanization, followed by the necropsy, the head from each mouse was removed from the carcass and the lower jaw, skin, muscles, eyes and dorsal cranium were detached. The anterior cranium was then immersed in 4% formaldehyde and stored for 24 h for fixation. Following fixation, the anterior craniums were decalcified in a 10% EDTA (pH = 7.2) solution for 3 days in an oven set at 37 °C , then rinsed in distilled water followed by standard histological routine processing for paraffin embedding. One paraffin block containing the whole head was made for each mouse, and four specific anatomical locations were selected for light microscopy, following the methodologies of Young (1981) and Corps et al. (2010).

Briefly, the proximal section (T1) was sectioned immediately caudal to the upper incisive teeth; the middle section (T2) was sectioned at the level of the incisive papilla of the hard palates; the third nasal section (T3) was sectioned at the level of the second palatal ridge; and the most caudal nasal section (T4) was sectioned at the level of the intersection of the hard and soft palates (Fig. 2).

We made two sets of histological slides. Each set contained four slides (one slide of each T region) with several 4 µm thickness sections of each *M. musculus*. One set of slides was stained with haematoxylin and eosin (Martoja and Martoja-Pierson, 1970), as a standard procedure for general tissue architecture observation and comparisons; and the other set was stained with Alcian blue (pH 2.5)/periodic acid Schiff (AB/PAS) to identify acidic and neutral mucous substances stored in mucus-secreting cells of the airway surface epithelium, of the cells underlying the lateral nasal glands (LaNaGl) and of the Bowman's gland cells (BowGl).

Epithelium thickness measurements

Measurements of the respiratory epithelium (ResEpi) and olfactory epithelium (OlfEpi) were taken in all sections (T1, T2, T3 and T4) with the AB/PAS staining. Squamous epithelium (SquEpi) was only measured in T1 since it is only present in this section. These measurements were taken with a 200 × magnification.

For each individual, two areas of each type of epithelium were selected for the measurements, one on the right side of the nasal cavity and the other on the left. Five measurements were taken in each part of the epithelium selected from the basal lamina to the top of the cilia (T2, T3 and T4) or the upper layer of the squamous epithelium (T1).

Density of cell types in the olfactory epithelium

The density of cell types (basal, support and neuron cells) in the olfactory epithelium was performed in section T3, on the lining of the second ethmoid turbinate. The slides stained with H&E were used for these measurements since it is more appropriate to distinguish the nuclei of basal cells, support cells and olfactory receptor neurons. The distinction of these cellular types was based on the location of the nuclei:

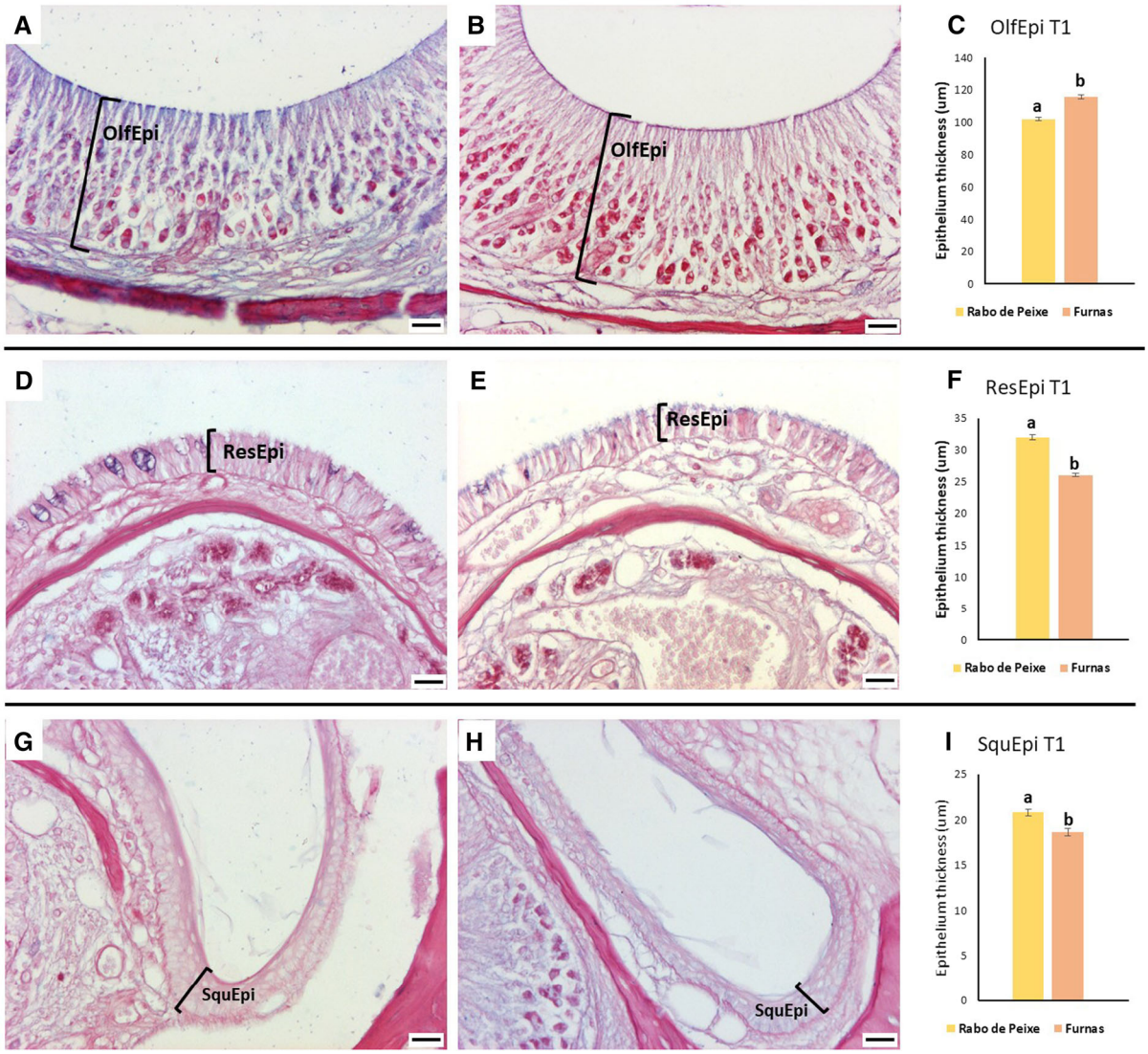

Fig. 3 Epithelial morphometric measurements of OlfEpi, ResEpi and SquEpi on section T1 of mice captured at: Rabo de Peixe (**a**, **b**, **g**) and Furnas (**b**, **e**, **h**). Histograms representing the mean epithelial thickness measurements of the OlfEpi-T1 **c**; ResEpi-T1 **d** and SquEpi-T1 **e**. Bars represent the standard errors. Locations with different letters are significantly different at $p = 0.05$ (Student's t-test). Scale bars = 25 µm

nuclei from support cells are aligned in a single apical row through the epithelium, nuclei from basal cells are found lying just on top of the lamina propria, and all the nuclei in the middle-upper layers correspond to the olfactory receptor neurons (Murdoch & Roskams, 2007). Cell type counting in section T3 was performed within a selected area of the epithelium (mean = 8732,8 μm^2, minimum = 5680,3 μm^2 and maximum = 12,614,3 μm^2 values of the measured areas), using a 400 × magnification. Six areas were measured per individual, three on the left side and three on the right side.

Area measurements in the lateral nasal glands

Measurements of the surface of the LaNaGl were taken in T3 slides stained with AB/PAS, with a 25 × magnification. From each gland section, the total area was measured, along with the serous area (PAS + +) and the mucous one (PAS ±). Two

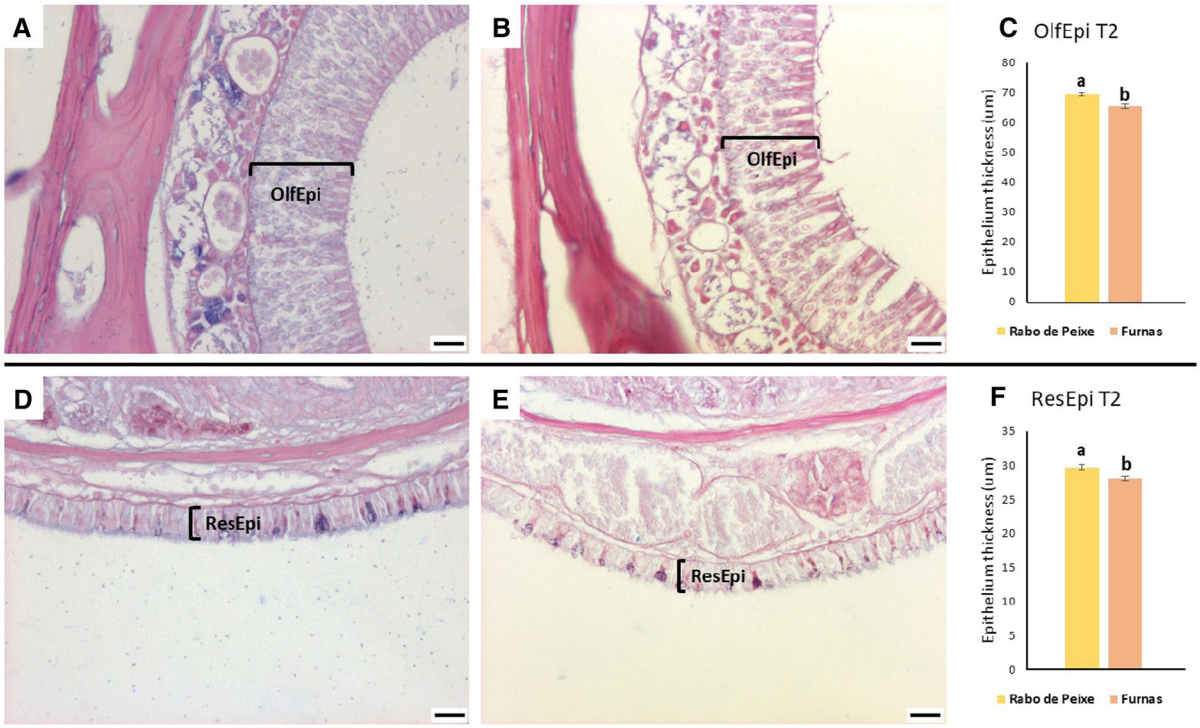

Fig. 4 Epithelial morphometric measurements of OlfEpi and ResEpi on section T2 of mice captured at: Rabo de Peixe (**a**, **b**) and Furnas (**b**, **e**). Histograms representing the mean epithelial thickness measurements of the OlfEpi-T2 **c** and ResEpi-T2 **d**. Bars represent the standard errors. Locations with different letters are significantly different at $p = 0.05$ (Student's t-test). Scale bars = 25 µm

measurements were obtained per individual, one on the left gland and the other on the right gland. Both the serous (PAS + +) and the mucous (PAS ±) areas were calculated separately and a ratio of proportions [(PAS + +)/(PAS ±)] was then calculated.

Secretory activity of the Bowman's glands, goblet cells and lateral nasal glands

Photographs of the lamina propria under the OflEpi, taken at a 200 × magnification, were made in all individuals to observe the activity of the BowGls.

A semi-quantitative evaluation of the BowGls activity was performed by stain intensity and scored 1 to 3: 1—low activity: no mucus AB/PAS stained (see Fig. 8a); 2—medium activity: mucus mildly AB/PAS stained (see Fig. 8b); 3—high activity: mucus intensely AB/PAS stained (see Fig. 8c). The secretory activity of the goblet cells (GobCells) within the respiratory epithelium was also observed and scored in the same way as BowGls. Additionally, the distribution of the GobCells in the respiratory epithelium was evaluated and scored as follows: 1—< 20% of the area of ResEpi occupied by GobCells, 2—21–50% of the area of ResEpi occupied by GobCells, 3—> 50% of the area of ResEpi occupied by GobCells. Finally, the activity of the serous part of the LaNaGl was also evaluated and scored as follows: 1—< 20% of the cells with the cytoplasm full of secretory granules (see Fig. 7f); 2—21–80% of the cells with the cytoplasm full of secretory granules (see Fig. 7g); 3—> 80% of the cells with the cytoplasm full of secretory granules (see Fig. 7h)]. For all these evaluations in the T3, the AB/PAS slides were used.

All measurements were taken using the software Image Pro-Plus 5.0 by MediaCybernetics® connected to a Leica® DM1000 microscope (Cambridge, UK).

Statistical analysis

Statistical analysis was performed using SPSS version 25.0 (SPSS Inc., Chicago, IL, USA). All the quantitative data were analysed using the Student's t-test, and when required, data were transformed by SQRT

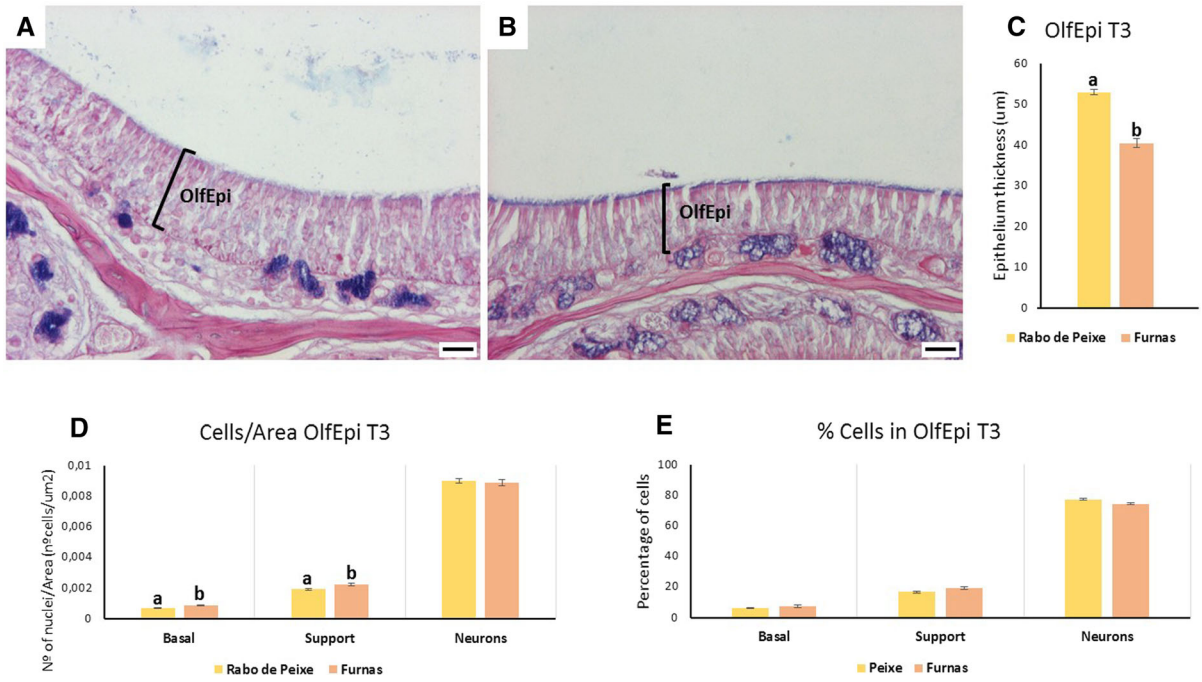

Fig. 5 Epithelial morphometric measurements of OlfEpi at T3 of mice captured at: **a** Rabo de Peixe and **b** Furnas. Histograms representing the mean epithelial thickness measurements of the OlfEpi-T3 **c**; bars represent the standard errors. Locations with different letters are significantly different at $p = 0.05$ (Student's t-test). Histograms representing the differences on the density of cell types in OlfEpi-T3 **d** and the percentage of each cell type in OlfEpi-T3 **e**; locations with different letters are significantly different at $p = 0.05$ (Mann–Whitney test). Scale bars = 25 µm

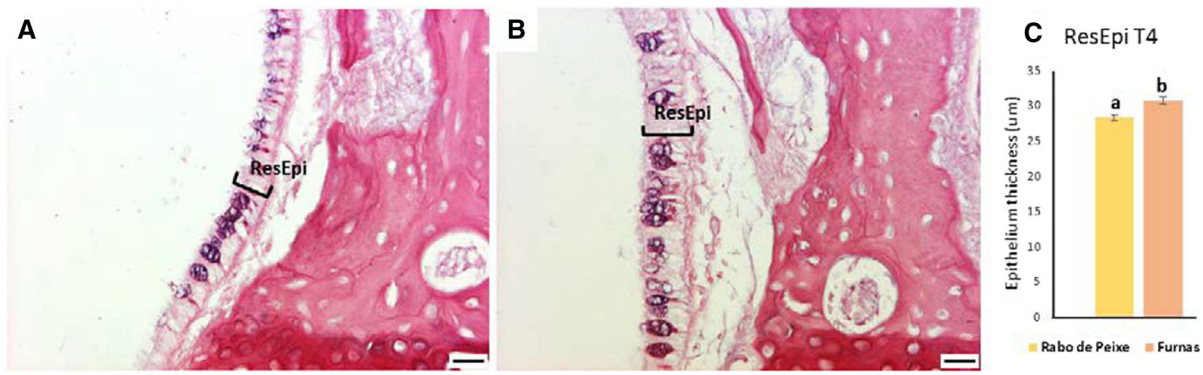

Fig. 6 Epithelial morphometric measurements of ResEpi at T4 of mice captured at: **a** Rabo de Peixe and **b** Furnas. Histograms representing the mean epithelial thickness measurements of the ResEpi-T4 **c**. Bars represent the standard errors. Locations with different letters are significantly different at $p = 0.05$ (Student's t-test). Scale bars = 25 µm

(x + 0.5) to normalize the data. For the semi-quantitative data, the Mann–Whitney was used. The level of significance was set at $p \leq 0.05$.

Results

The sex ratio of mice captured at both locations was similar (≈50%). No significant differences were found in the weight of mice from both locations (13.59 ± 0.93 g, Furnas; 13.47 ± 0.46 g, Rabo de Peixe; t(28) = 0.14; $p = 0.893$) as well as in their age

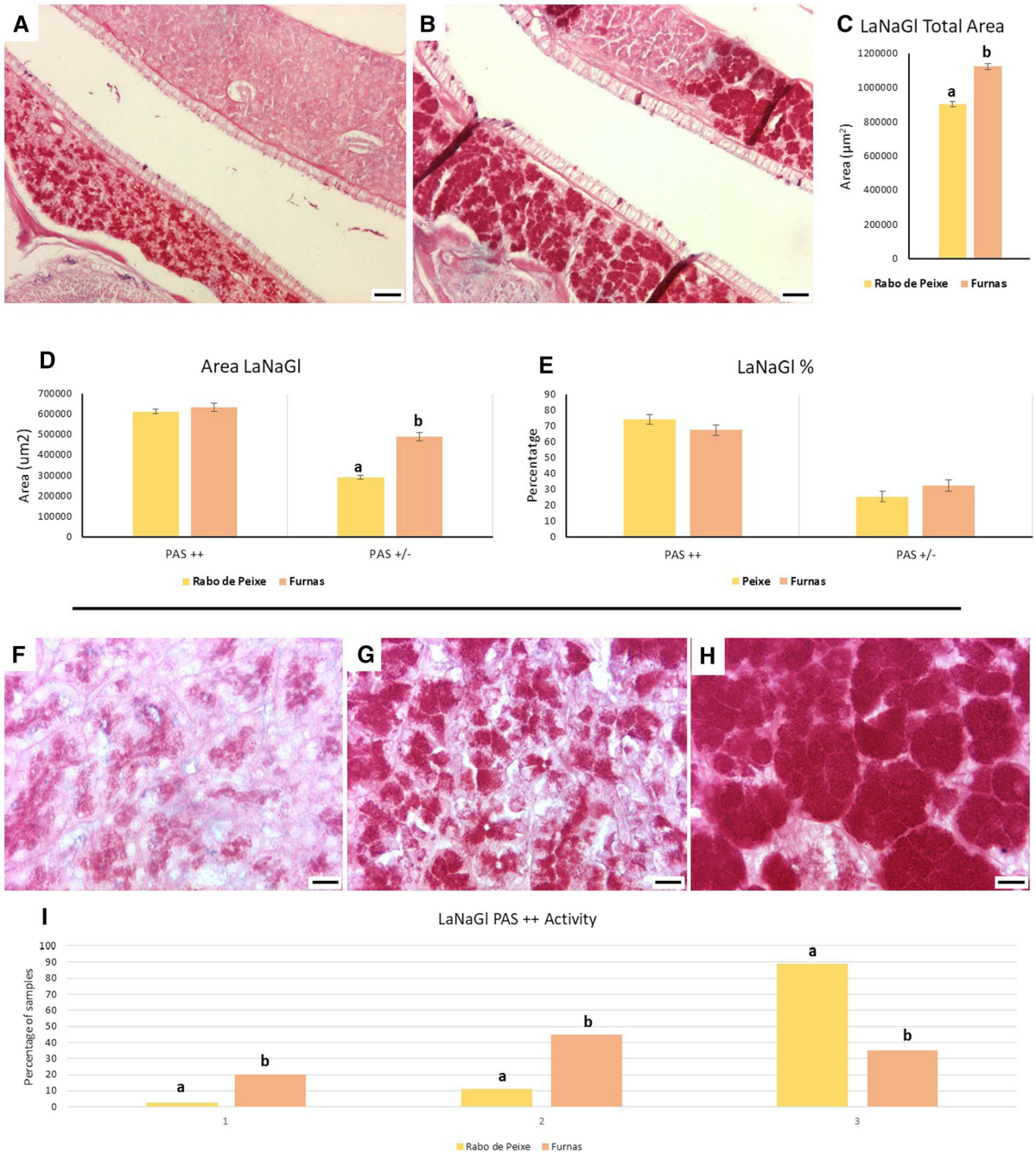

Fig. 7 Histograms representing the total area of the LaNaGl (C), areas of serous part (PAS + +) and the mucous part (PAS ±) (D) and the relative area of serous part (PAS + +) and the mucous part (PAS ±) (E) of mice captured at: A—Rabo de Peixe and B—Furnas. Locations with different letters are significantly different at $p = 0.05$ [C, D and E (Student's t-test)]. Histogram representing the activity of the LaNaGl (I). The magnitude of the activity has been classified in 3 levels: 1—< 20% of the cells with the cytoplasm full of secretory granules (F); 1—20–80% of the cells with the cytoplasm full of secretory granules (G); and 3—> 80% of the cells with the cytoplasm full of secretory granules (H). Locations with different letters are significantly different at $p = 0.05$ (Mann–Whitney test). Scale bars: (A and B) = 250 µm; (F, G and H) = 15 µm

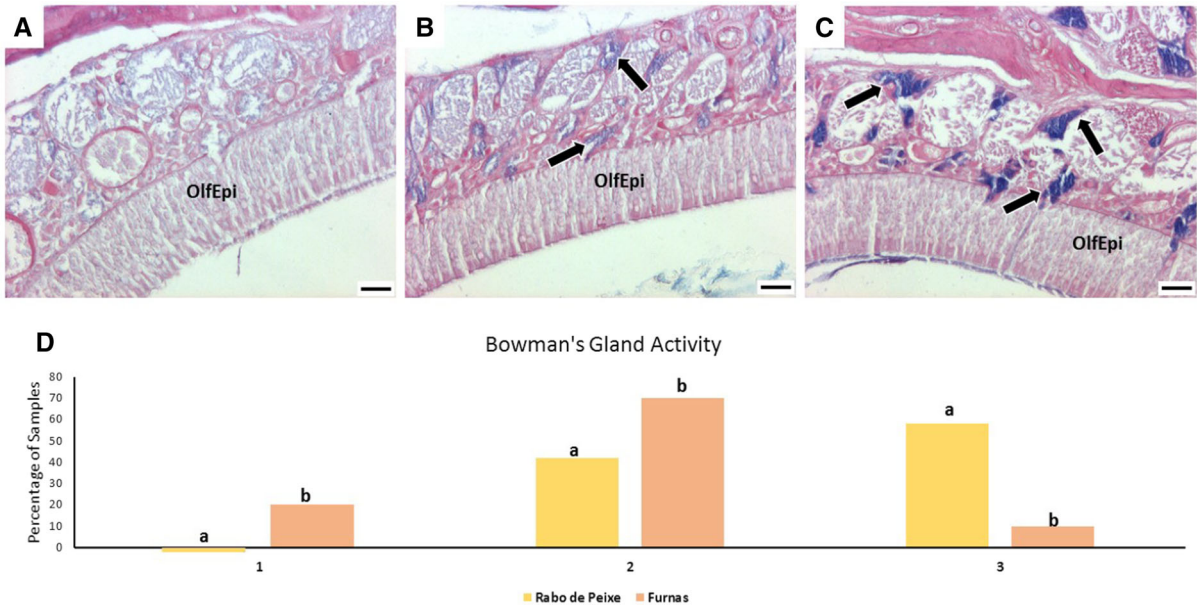

Fig. 8 Histograms representing the distribution of the levels of activity of the BowGl (D), located under the OlfEpi-T3. The activity has been classified in 3 levels: low activity, no mucus AB/PAS stained **a**; 2—medium activity, mucus mildly AB/PAS stained **b**; 3—high activity, mucus intensely AB/PAS stained **c**. Black arrows represent the Bowman's Gland secretory unit. Locations with different letters are significantly different at $p = 0.05$ (Mann–Whitney test). Scale bars = 25 µmF

(178 ± 25 days, Furnas; 220 ± 14 days, Rabo de Peixe; t(28) = − 1.60; $p = 0.12$).

Epithelium thickness

Section T1: The OlfEpi-T1 was significantly thicker in mice from Furnas when compared to Rabo de Peixe (115.94 ± 1.32 µm and 102.28 ± 1.11 µm, respectively, t(278) = − 5.729, $p < 0.001$; Fig. 3a, b and c). The ResEpi-T1 was significantly thinner in mice from Furnas when compared to Rabo de Peixe (26.13 ± 0.30 µm and 32.02 ± 0.41 µm, respectively, t(288) = 8.426, $p < 0.001$; Fig. 3d, e and f) as well as the SquEpi-T1 (18.72 ± 0.41 µm and 20.84 ± 0.36 µm, respectively, t(283) = 3.080, $p = 0.002$, Fig. 3g, h and i).

Section T2: The OlfEpi-T2 was significantly thinner in mice from Furnas when compared to Rabo de Peixe (65.66 ± 0.69 µm and 69.57 ± 0.42 µm, respectively, t(286) = 3.808, $p < 0.001$; Fig. 4a, b and c) as well as the ResEpi-T2 (28.17 ± 0.35 µm and 29.73 ± 0.38 µm, respectively, t(288) = 2.071, $p = 0.039$; Fig. 4d, e and f).

Section T3: The OlfEpi-T3 was significantly thinner in mice from Furnas when compared to Rabo de Peixe (40.44 ± 1.09 µm and 53.00 ± 0.62 µm, respectively, t(253) = 8.377, $p < 0.001$; Fig. 5a, b and c). The thickness of ResEpi-T3 did not present significant differences between the studied groups ($p > 0.05$, t test; SM—Table 1).

Section T4: The thickness of OlfEpi-T4 did not differ significantly between the studied groups ($p > 0.05$, t test; SM—Table 1). The ResEpi-T4 was significantly thicker in mice from Furnas when compared to Rabo de Peixe (30.74 ± 0.49 µm and 28.31 ± 0.36 µm, respectively, t(238) = − 4.093, $p < 0.001$; Fig. 6a, b and c).

Density of cell types in the olfactory epithelium (T3)

The number of basal cells per area (µm^2) at OlfEpi-T3 was significantly higher in mice from Furnas when compared to Rabo de Peixe ($8.54 \times 10^{-4} \pm 3.41 \times 10^{-5}$ and $7.01 \times 10^{-4} \pm 2.19 \times 10^{-5}$, respectively, t(147) = − 3.736, $p < 0.001$; Fig. 5d), as well as the number of support cells per area (µm^2) ($2.00 \times 10^{-3} \pm 9.91 \times 10^{-5}$ and $1.91 \times 10^{-3} \pm 5.05 \times 10^{-5}$, respectively, t(147) = − 2.648, $p = 0.010$; Fig. 5d). However, the number of olfactory

neurons per area (μm^2) at OlfEpi-T3 did not differ significantly between both studied groups ($p > 0.05$, *t* test; Fig. 5d, SM—Table 1).

Area of the lateral nasal glands

The LaNaGl total area (μm^2) was significantly larger in mice from Furnas when compared to Rabo de Peixe (1,144,183 ± 34,691 and 1,006,604 ± 25,627, respectively, t(272) = − 5.796, $p < 0.001$; Fig. 7a, b and c).

The PAS ± portion area of the LaNaGl was significantly larger in the mice from Furnas when compared to Rabo de Peixe (527,740.5 ± 35,241.58 and 431,340.3 ± 25,900.67, respectively; t(207) = − 2.201, $p = 0.029$; Fig. 7d). The area of the PAS + + portion of the LaNaGl did not differ significantly between both studied groups ($p > 0.05$; Fig. 7d, SM—Table 1). The relative percentage of area occupied by the serous part (PAS + +) and percentage of area occupied by mucous part (PAS ±) in the LaNaGl did not differ significantly between studied groups ($p > 0.05$; Fig. 7e).

Secretory activity of the Bowman's glands, goblet cells and lateral nasal glands

The distribution of the levels of activity in BowGl was significantly different between both mice groups ($U = 41.50$, $p = 0.012$, Fig. 8), being lower in Furnas (Mdn = 2) when compared to Rabo de Peixe (Mdn = 3).

The level of activity of GobCells did not differ significantly between both studied groups ($U = 2487$, $p = 0.005$).

The level of activity of PAS + + in the LaNaGl was significantly lower in mice from Furnas (Mdn = 2) when compared to Rabo de Peixe (Mdn = 3) ($U = 35.50$, $p = 0.005$; Fig. 7f, g, h and i).

Discussion

Several studies in mice have revealed a link between the inhalation of toxins and neurotoxic, inflammatory and mucosecretory responses in the nasal airways (Camargo Pires-Neto et al., 2006; Chamanza & Wright, 2015; Corps et al., 2010; Harkema et al., 2006; Islam et al., 2006). Despite the previously found evidence about the hazardous consequences of chronic exposure to volcanogenic air pollution in humans (Amaral et al., 2006, 2008; Linhares et al., 2015; Rodrigues et al., 2012; Tam et al., 2016) and animals (Amaral & Rodrigues, 2011; Amaral et al., 2007b; Camarinho et al., 2013; Camarinho et al., 2019a; Camarinho, et al., 2019b), no study has ever been conducted in the nasal cavity.

In this study, we evaluated several morphometric parameters of the nasal cavity epithelium and the mucosecretory responses of the mucosal glands. Overall, our results showed that the mice captured in the volcanically active environment (Furnas Village) presented concerning values in histomorphometrical data and mucosecretory activity. Our results clearly showed a thinner respiratory and squamous epithelium (T1) in Furnas individuals (Figs. 3 and 4), particularly in T1 and T2 sections. However, in T4 the ResEpi was significantly thicker in Furnas mice. These results pinpoint a possible higher impact of the hazardous pollutants on the anterior region of the nasal cavity (T1 and T2) rather than the posterior one (T4).

The GobCells are found within the ResEpi and their major function is to lubricate and protect the epithelium (Jaramillo et al., 2018; Thornton et al., 2008). Previous studies have found that chronic exposure to irritant substances or compounds causes hypersecretion of GobCells (Rogers, 2007; Thornton et al., 2008; Widdicombe & Wine, 2015), but the glands responses depend on the type of irritant substance or compound. Nevertheless, our results showed no differences in the secretory activity of the GobCells between both sites. This difference could be because the complex mixture of air pollutants present at hydrothermal emissions is distinct from the air pollutants of anthropogenic source or smoking activity. Nonetheless, since that the ResEpi in mice from Furnas was generally thinner, GobCells are most probably smaller and thus the total mucus volume secreted would be inferior in Furnas individuals. Less mucous secretion could represent a higher exposure of the epithelium to toxics, which in turn causes more damages that are translated into a thinner epithelium, leading, again, to less mucus volume and so on, creating a loop of negative effects.

The OlfEpi showed an opposite tendency since it was possible to find more severe differences in the T3 posterior region, but also affecting T2 (Figs. 4, 5). Mice from Furnas were exposed to hydrothermal emissions that consist mainly of gases. These gases

could have a higher impact in these distal sections of the nasal cavity since they reach more easily the posterior regions. Such gases might alter the pH or dissolve into the mucus causing cellular damage and toxicity in these deeper areas of the nasal cavity. Such hypothesis is reinforced by the significantly lower thickness of the OlfEpi found in Furnas' mice in T2 and T3 (Figs. 4, 5) since these mice were chronically exposed to hydrothermal emissions (considered to be an acidic environment). The fact that these effects did not extend to T4, deeper in the nasal cavity, might have to do with the gases' ability to be dissolved on the way and, consequently, the concentrations that reach T4 are too low to cause toxicity.

Atrophy of the OlfEpi after chronic exposure to inhaled toxicants has already been reported by Corps et al. (2010) and Harkema et al. (2006). However, in this study, the OlfEpi in the T1 section behaved contrarily to the other sections. T1 epithelium was thicker in Furnas individuals and, the epithelium of the other sections (T2–4) was thicker in Rabo de Peixe individuals. Despite these differences, in both populations, the OlfEpi in T1 was thicker than in the other sections (almost twice the thickness). The fact that the T1 epithelium is thicker in Furnas can be explained by two proposed mechanisms: (i) A negative feedback—mice from Rabo de Peixe inhabit near quarries (Amaral et al., 2007b), therefore they could be exposed to increased amounts of PM_{10} (Particulate Matter $\leq$ 10 μm) and $PM_{2,5}$ (Particulate Matter $\leq$ 2,5 μm) that could affect primarily the anterior region (T1) and thus reduce the thickness of its OlfEpi. In this case scenario, the epithelium from Furnas would be considered "normal" when compared to mice from Rabo de Peixe (in which the PM exposure would cause a thinner epithelium); (ii) A positive feedback—the presence of high volumes of gases from the hydrothermal emissions (e.g. H_2S, CO_2, ^{222}Rn) might have affected the sensorial cells of the mice from Furnas, meaning that the OlfEpi of the vomeronasal organ (VomOrg) by being overloaded with several toxic gases, tends to proliferate to compensate the diminishing olfactory capacity (thus resulting in a thicker OlfEpi). The VomOrg is an olfactive organ present in some animals (not present in humans) to sense pheromones, and it possesses some cellular and structural differences. Unlike the OlfEpi from the remaining areas, the OlfEpi from the VomOrg does not have a basal cell layer, and its neurons do not have cilia (Chamanza & Wright, 2015). Although the first proposed hypothesis cannot be completely ruled out, the second hypothesis is consistent with the observations of Chamanza and Wright (2015), who detected basal cell hyperplasia in the OlfEpi that had been prolongedly injured.

The number of nuclei of basal and support cells per area was significantly higher in the OlfEpi (T3 section) from Furnas' mice when compared to the Rabo de Peixe (Fig. 5). Such results suggest that these cells have a greater cellular turnover in Furnas individuals, since that the basal cells serve as the stem cells for the support cells and the olfactory neurons (Chamanza & Wright, 2015). This might also be an indicator of a high cell proliferation rate, possibly explaining the differences in the density of neurons in the OlfEpi between the studied sites. Given that one of the functions of support cells is to protect the neurons, this might be the reason they were replicating faster in the mice from Furnas. Despite this fact, the OlfEpi was thinner in Furnas (Fig. 5), which could also be the result of an inferior number of neurons. A loss in the number of olfactory sensory neurons was also observed by Islam et al. (2006) in nasal epithelium from mice exposed to satratoxin G. Therefore, to fully understand such effects, we developed a Functional Olfactory Index (FOI), being FOI = (n° neurons/Area) /Mean of Epithelium thickness). The resulting calculated FOIs for the mice from Rabo de Peixe and Furnas were 0.476 and 0.359, respectively, reflecting a possible loss in the capacity of olfaction in mice from Furnas (despite the fact of the probably higher cell proliferation rate in the OlfEpi of Furnas' mice).

The BowGls from Furnas' mice were not as active as those from Rabo de Peixe [Fig. 8; Mdn = 3 (Rabo de Peixe), Mdn = 2 (Furnas)]. One of the functions of these glands is to dissolve the odorants before they contact the cilia of the olfactory neurons, meaning that a decreased secretion could contribute to a loss of olfaction (Jafari et al., 2010). Both facts combined [(the decrease in BowGl secretion and the decrease in the number of neurons in the individuals from Furnas (according to the calculated FOI)], might produce a synergic effect resulting in a loss of olfactory capacity. It is also possible that the GEM inhalation could have a negative effect in the olfactory neurons, since that Hg is neurotoxic. In fact, Navarro-Sempere et al. (2020) found much more mercury deposits in the brain blood vessels, white matter and some cells of the

hippocampus of mice chronically exposed to the hydrothermal emissions of Furnas volcano than in the individuals not exposed. Similarly, Camarinho et al., 2021 found a large abundance of Hg deposits in the lungs of mice captured at Furnas Village, while no presence of Hg was observed in mice captured at Rabo de Peixe. These combined results of these studies suggest that there is a possibility that the olfactory neurons could be affected through direct damage during inhalation or indirect damage, through the bioaccumulation of GEM in the lung that then enters the bloodstream causing toxicity to other organs. Future studies should be considered in this particular matter, since that the several mechanisms involved in both possibilities are yet unclear.

The LaNaGl possesses two components: PAS + + (serous) and PAS ± (mucous), which exhibit different properties. The serous secretion contains bactericidal and antimicrobial agents, while mucous secretion creates a gel on the surface of the epithelium to maintain a proper viscosity and might contain antimicrobial agents (Chamanza & Wright, 2015; Widdicombe & Wine, 2015). The LaNaGl were 20% larger in mice from Furnas when compared to mice from Rabo de Peixe, but only the mucous component (PAS ±) presented hypertrophy in Furnas mice (Fig. 7). However, the relative percentage of the mucous component (PAS ±) concerning the total area of the gland was not significantly different between the two studied populations. Even though the serous part (PAS + +) did not differ significantly in size, its activity (secretion) was significantly higher in mice from Rabo de Peixe than in mice from Furnas. On average, our results show that more than 80% of cells presented the cytoplasm full of secretory granules in mice from Rabo de Peixe, but in mice from Furnas, the average of cells with the cytoplasm full of secretory granules was between 21 and 80%. We calculated the amount of secretion (Serous Area*Activity mean), and we concluded that it was 23% higher in mice from Rabo de Peixe. Our data is consistent with the findings of Widdicombe and Wine (2015) that revealed that individuals suffering from chronic bronchitis, because of persistent irritation, presented inflammation and an increase in the gland size. Some studies have already linked chronic exposure to volcanic activity in Furnas with chronic bronchitis in humans and mice (Amaral et al., 2007a; Camarinho et al., 2019b), making the combined results of the previous studies consistent with the larger mucous component observed in mice from Furnas. Another study in mice nasal cavity by Corps et al. (2010) also described hypersecretion of the LaNaGl from mice exposed to intranasal instillation of roridin A toxin; however, in this study, no distinction was made between the two types of secretion. Regarding the serous activity of the LaNaGl, it is possible that the hazardous properties of the hydrothermal emissions directly affect the serous cells, causing atrophy in the serous component. Furthermore, Fukuda et al. (2008) described that knockout mice for the receptors responsible for the secretion of the LaNaGl showed nasal inflammation and a decrease in olfactory capacity. These consequences of the LaNaGl misfunction could cause a synergic effect with the lower number of olfactory neurons and the lower secretion activity of BowGls observed in Furnas' mice, ultimately leading to a loss of the capacity of olfaction. In addition, the inferior serous secretion activity of the LaNaGl in mice from Furnas could have left the lower airways more exposed to the effects of air contaminants, causing inflammation and extensive damage in the mice lungs, as observed in other previous studies (Camarinho et al., 2019a, b).

Conclusions

This study showed the hazardous potential of hydrothermal emissions on the respiratory and olfactory epithelia of the nasal cavity. Results showed that non-eruptive active volcanism clearly alters the histomorphometry of the nasal cavity in mice. The atrophy presented in the three analysed epithelia along with the altered mucosal components could leave the lower airways more vulnerable to air pollutants, making the individuals from Furnas more susceptible to develop respiratory pathologies. These individuals could also be suffering the loss of olfactory capabilities due to the observed differences in the cell types of the olfactory epithelium. The results of this study revealed the necessity to further study these effects in humans that are chronically exposed to air pollutants in hydrothermal areas.

Acknowlegements The authors would like to thank Paulo Melo for the field assistance in the capture of *Mus musculus*. Ricardo Camarinho is currently supported by a Ph.D. fellowship

grant (M3.1.a/F/048/2015) from Fundo Regional da Ciência (Regional Government of the Azores).

Data availability The datasets used and/or analysed during the current study are available from the corresponding author on reasonable request.

Declarations

Conflicts of interest The authors declare that they have no conflicts of interest.

Ethical Approval All the procedures were carried out in strict accordance with the European Convention for the protection of vertebrate animals used in experimental and other scientific purposes (ETS123), directive 2010/63/EU and Portuguese law decree (DL 113/2013), and approved by the Ethics committee of the University of Azores (project 10/2020). All efforts were made to minimize animal suffering.

References

Amaral, A. F. S., Arruda, M., Cabral, S., & Rodrigues, A. S. (2008). Essential and non-essential trace metals in scalp hair of men chronically exposed to volcanogenic metals in the Azores. *Portugal. Environment International, 34*(8), 1104–1108. https://doi.org/10.1016/j.envint.2008.03.013

Amaral, A., Cabral, C., Guedes, C., & Rodrigues, A. (2007). Apoptosis, metallothionein, and bioavailable metals in domestic mice (Mus musculus L.) from a human-inhabited volcanic area. *Ecotoxicology, 16*, 475–482. https://doi.org/10.1007/s10646-007-0156-y

Amaral, A. F. S., & Rodrigues, A. S. (2007). Chronic exposure to volcanic environments and chronic bronchitis incidence in the Azores. *Portugal. Environmental Research, 103*(3), 419–423. https://doi.org/10.1016/j.envres.2006.06.016

Amaral, A. F. S., & Rodrigues, A. S. (2011). Volcanogenic contaminants: Chronic exposure. In J. Nriagu (Ed.), *Encyclopedia on Environmental Health* (pp. 681–689). Elsevier B.V.

Amaral, A., Rodrigues, V., Oliveira, J., Pinto, C., Carneiro, V., Sanbento, R., Cunha, R., & Rodrigues, A. (2006). Chronic exposure to volcanic environments and cancer incidence in the Azores, Portugal. *Science of the Total Environment, 367*, 123–128. https://doi.org/10.1016/j.scitotenv.2006.01.024

Bagnato, E., Viveiros, F., Pacheco, J. E., D'Agostino, F., Silva, C., & Zanon, V. (2018). Hg and CO2 emissions from soil diffuse degassing and fumaroles at Furnas Volcano (São Miguel Island, Azores): Gas flux and thermal energy output. *Journal of Geochemical Exploration, 190*, 39–57.

Camargo Pires-Neto, R., Júlia Lichtenfels, A., Regina Soares, S., Macchione, M., Saldiva, H. N., & P., Dolhnikoff, M. . (2006). Effects of São Paulo air pollution on the upper airways of mice. *Environmental Research, 101*(3), 356–361. https://doi.org/10.1016/j.envres.2005.12.018

Camarinho, R., Garcia, P. V., Choi, H., & Rodrigues, A. S. (2019a). Chronic exposure to non-eruptive volcanic activity as cause of bronchiolar histomorphological alteration and inflammation in mice. *Environmental Pollution, 253*, 864–871. https://doi.org/10.1016/j.envpol.2019.07.056

Camarinho, R., Garcia, P. V., Choi, H., & Rodrigues, A. S. (2019b). Overproduction of TNF-α and lung structural remodelling due to chronic exposure to volcanogenic air pollution. *Chemosphere, 222*, 227–234.

Camarinho, R., Garcia, P. V., & Rodrigues, A. S. (2013). Chronic exposure to volcanogenic air pollution as cause of lung injury. *Environmental Pollution, 181*, 24–30. https://doi.org/10.1016/j.envpol.2013.05.052

Camarinho, R., Navarro-Sempere, A., Garcia, P. V., García, M., Segovia, Y., & Rodrigues, A. S. (2021). Chronic exposure to volcanic gaseous elemental mercury: Using wild Mus musculus to unveil its uptake and fate. *Environmental Geochemistry and Health*. https://doi.org/10.1007/s10653-021-00924-z

Chamanza, R., & Wright, J. A. (2015). A review of the comparative anatomy, histology, physiology and pathology of the nasal cavity of rats, mice, dogs and non-human primates. Relevance to inhalation toxicology and human health risk assessment. *Journal of Comparative Pathology, 153*(4), 287–314.

Coakley, R. J., Taggart, C., Greene, C., McElvaney, N. G., & O'Neill, S. J. (2002). Ambient pCO2 modulates intracellular pH, intracellular oxidant generation, and interleukin-8 secretion in human neutrophils. *Journal of Leukocyte Biology, 71*, 603–610.

Corps, K. N., Islam, Z., Pestka, J. J., & Harkema, J. R. (2010). Neurotoxic, inflammatory, and mucosecretory responses in the nasal airways of mice repeatedly exposed to the macrocyclic trichothecene mycotoxin Roridin A: dose-response and persistence of injury. *Toxicologic Pathology, 38*(3), 429–451. https://doi.org/10.1177/0192623310364026

Fukuda, N., Shirasu, M., Sato, K., Ebisui, E., Touhara, K., & Mikoshiba, K. (2008). Decreased olfactory mucus secretion and nasal abnormality in mice lacking type 2 and type 3 IP3 receptors. *European Journal of Neuroscience, 27*(10), 2665–2675. https://doi.org/10.1111/j.1460-9568.2008.06240.x

Guest, J. E., Gaspar, J. L., Cole, P. D., Queiroz, G., Duncan, A. M., Wallenstein, N., Ferreira, T., & Pacheco, J. M. (1999). Volcanic geology of Furnas volcano, São Miguel, Azores. *Journal of Volcanology and Geothermal Research, 92*(1–2), 1–29.

Hansell, A., & Oppenheimer, C. (2004). Health hazards from volcanic gases: A systematic literature review. *Archives of Environmental Health, 59*, 628–639. https://doi.org/10.1080/00039890409602947

Harkema, J. R., Carey, S. A., & Wagner, J. G. (2006). The nose revisited: A brief review of the comparative structure, function, and toxicologic pathology of the nasal epithelium. *Toxicologic Pathology, 34*(3), 252–269. https://doi.org/10.1080/01926230600713475

Hendry, J. H., Simon, S. L., Wojcik, A., Sohrabi, M., Burkart, W., Cardis, E., Laurier, D., Timarche, M., & Hayata, I. (2009). Human exposure to high natural background

radiation: What can it teach us about radiation risks? *Journal of Radiological Protection, 29*, A29–A42.

International Agency for Research on Cancer Monographs on the evaluation of the carcinogenic risks to Humans (IARC). (1988). Man-made mineral fibres and radon. *Lyon, France: IARC Press, 43*, 33–171.

Islam, Z., Harkema, J. R., & Pestka, J. J. (2006). Satratoxin G from the black mold Stachybotrys chartarum evokes olfactory sensory neuron loss and inflammation in the murine nose and brain. *Environmental Health Perspectives, 114*(7), 1099–1107. https://doi.org/10.1289/ehp.8854

Jafari, F.H., Minhas, L.A., Shoro, A.A., Tahir, M. (2010). A histological study of bowman's glands in humans olfactory Mucosa. Pakistan Armed Forces Medical Journal, 60(1), 3–8. Available from: https://www.researchgate.net/publication/271509372_A_HISTOLOGICAL_STUDY_OF_BOWMAN'S_GLANDS_IN_HUMAN_OLFACTORY_MUCOSA

Jaramillo, A. M., Azzegagh, Z., Tuvim, M. J., & Dickey, B. F. (2018). Airway mucin secretion. *Annals of the American Thoracic Society, 15*, 164–170. https://doi.org/10.1513/AnnalsATS.201806-371AW

Kristbjornsdottir, A., & Rafnsson, V. (2013). Cancer incidence among population utilizing geothermal hot water: A census-based cohort study. *International Journal of Cancer, 133*, 2944–2952.

Linhares, D., Garcia, P. V., Garcia, F., Ferreira, T., Rodrigues, A. D. S. (2015). Air pollution by hydrothermal volcanism and human pulmonary function. *BioMed Research International*, *2015*, 326794. https://doi.org/10.1155/2015/326794.

Linhares, D., Garcia, P., Rodrigues, A. (2017). Radon exposure and human health: What happens in volcanic environments? In F. Adrovic (Ed.). Radon. doi: https://doi.org/10.5772/intechopen.71073.

Linhares, D., Garcia, P. V., Silva, C., Barroso, J., Kazachkova, N., Pereira, R., Lima, M., Camarinho, R., Ferreira, T., & Rodrigues, A. (2018). DNA damage in oral epithelial cells of individuals chronically exposed to indoor Radon (222Rn) in a hydrothermal área. *Environmental Geochemistry and Health, 40*(5), 1713–1724.

Martoja, R., Martoja-Pierson, M., Grumbles, L. C., Moncanut, M. E., & Coll, M. D. (1970). *Técnicas de histologia animal* (1st ed.). Toray-Masson.

Maynard, R., Krzyzanowski, M., Vilahur, N., Héroux, M.-E. (2017). Evolution of WHO air quality guidelines: past, present and future. Copenhagen: WHO Regional Office for Europe. Available from: http://www.euro.who.int/en/health-topics/environment-and-health/air-quality/publications/2017/evolution-of-who-air-quality-guidelines-past,-present-and-future-2017

Murdoch, B., & Roskams, A. J. (2007). Olfactory epithelium progenitors: Insights from transgenic mice and in vitro biology. *Journal of Molecular Histology, 38*(6), 581–599. https://doi.org/10.1007/s10735-007-9141-2

Navarro-Sempere, A., Segovia, Y., Rodrigues, A. S., Garcia, P. V., Camarinho, R., & García, M. (2020). First record on mercury accumulation in mice brain living in active volcanic environments: a cytochemical approach. *Environmental Geochemistry and Health., 43*(1), 171–183. https://doi.org/10.1007/s10653-020-00690-4

Quéré, J. P., & Vincent, J. P. (1989). Détermination de l'âge chez le mulot gris (Apodemus sylvaticus L., 1758) par la pesée des cristallins. *Mammalia, 53*, 287–294. https://doi.org/10.1515/mamm.1989.53.2.287

Rodrigues, A. S., Arruda, M. S. C., & Garcia, P. V. (2012). Evidence of DNA damage in humans inhabiting a volcanically active environment: A useful tool for biomonitoring. *Environment International, 49*, 51–56. https://doi.org/10.1016/j.envint.2012.08.008

Rogers, D.F. (2007). Physiology of airway mucus secretion and pathophysiology of hypersecretion. *Respiratory Care*, *52*(9), 1134–1146. Available from: http://rc.rcjournal.com/content/52/9/1134.

Searle, R. (1980). Tectonic pattern of the Azores spreading centre and triple junction. *Earth and Planetary Science Letters, 51*(2), 415–434.

Silva, C., Ferreira, T., Viveiros, F., & Allard, P. (2015). Soil radon (^{222}Rn) monitoring at Furnas Volcano (São Miguel, Azores): Applications and challenges. *European Physics Journal - Special Topics, 224*, 659–686.

Tam, E., Miike, R., Labrenz, S., Sutton, A. J., Elias, T., Davis, J., Chen, Y. L., Tantisira, K., Dockery, D., & Avol, E. (2016). Volcanic air pollution over the Island of Hawai'i: Emissions, dispersal, and composition. Association with respiratory symptoms and lung function in Hawai'i Island school children. *Environment International, 92–93*, 543–552. https://doi.org/10.1016/j.envint.2016.03.025

Thornton, D. J., Rousseau, K., & McGuckin, A. (2008). Structure and function of the polymeric mucins in airways mucus. *Annual Review of Physiology, 70*(1), 459–486.

Viveiros, F., Cardellini, C., Ferreira, T., Caliro, S., Chiodini, G., & Silva, C. (2010). Soil CO2 emissions at Furnas volcano, São Miguel Island, Azores archipelago: Volcano monitoring perspectives, geomorphologic studies, and land use planning application. *Journal of Geophysical Research: Solid Earth, 115*(12), 1–17.

Widdicombe, J. H., & Wine, J. J. (2015). Airway gland structure and function. *Physiological Reviews, 95*(4), 1241–1319. https://doi.org/10.1152/physrev.00039.2014

Young, J. T. (1981). Histopathological examination of the rat nasal cavity. *Fundamental and Applied Toxicology, 1*, 309–312. https://doi.org/10.1016/S0272-0590(81)80037-1